Anti-Inflammatory Effect of Gold Nanoparticles Supported on Metal Oxides

Takeshi Fujita (fujitatks@stf.teu.ac.jp)
Research Center for Gold Chemistry, Department of Applied Chemistry for Environment, Graduate School of Urban Environmental Sciences, Tokyo Metropolitan University, 1-1Minami-osawa, Hachioji, Tokyo 19

Maéva ZYSMAN
Univ Bordeaux, Centre de Recherche cardio-thoracique de Bordeaux, U1045, CIC 1401, Bordeaux,

Dan Elgrabli
SAS Naor Innov, Courbevoie

Toru Murayama
Research Center for Gold Chemistry, Department of Applied Chemistry for Environment, Graduate School of Urban Environmental Sciences, Tokyo Metropolitan University, 1-1Minami-osawa, Hachioji, Tokyo 19

Masatake Haruta
Research Center for Gold Chemistry, Department of Applied Chemistry for Environment, Graduate School of Urban Environmental Sciences, Tokyo Metropolitan University, 1-1Minami-osawa, Hachioji, Tokyo 19

Sophie Lanone
Univ Paris Est Creteil, INSERM, IMRB, F-94010 Creteil

Tamao Ishida
Research Center for Gold Chemistry, Department of Applied Chemistry for Environment, Graduate School of Urban Environmental Sciences, Tokyo Metropolitan University, 1-1Minami-osawa, Hachioji, Tokyo 19

Jorge Boczkowski
Univ Paris Est Creteil, INSERM, IMRB, F-94010 Creteil

Research Article

Keywords: nanoparticles (NPs), anti-inflammatory effect

Posted Date: February 26th, 2021

DOI: https://doi.org/10.21203/rs.3.rs-237217/v1

Version of Record: A version of this preprint was published at Scientific Reports on November 30th, 2021. See the published version at https://doi.org/10.1038/s41598-021-02419-4.

Anti-inflammatory effect of gold nanoparticles supported on metal oxides

Takeshi Fujita[1,2*], Maeva Zysman[3,4,5], Dan Elgrabli[3,6], Toru Murayama[1],
Masatake Haruta[1], Sophie Lanone[3], Tamao Ishida[1], Jorge Boczkowski[3,7*]

(1) Research Center for Gold Chemistry, Department of Applied Chemistry for Environment, Graduate School of Urban Environmental Sciences, Tokyo Metropolitan University, 1-1Minami-osawa, Hachioji, Tokyo 192-0397, Japan

(2) Department of Applied Chemistry, School of Engineering, Tokyo University of Technology, 1401-1Katakura, Hachioji, Tokyo192-0982, Japan

(3) Univ Paris Est Creteil, INSERM, IMRB, F-94010 Creteil, France

(4) Univ Bordeaux, Centre de Recherche cardio-thoracique de Bordeaux, U1045, CIC 1401, Bordeaux, France.

(5) Service des Maladies Respiratoires, CHU Bordeaux, Bordeaux, France

(6) SAS Naor Innov, Courbevoie, France

(7) AP-HP, Hopital Henri Mondor, Antenne de Pneumologie, F-94010 Creteil, France

** corresponding authors : fujitatks@stf.teu.ac.jp, jorge.boczkowski@inserm.fr*

ABSTRACT

Gold (Au) can be deposited as nanoparticles (NPs) smaller than 10 nm in diameter on a variety of metal oxide (MOx) NPs. Au/MOx NPs have high catalytic performance and selective oxidation capacity which could have implications in terms of biological activity, and more specifically in modulation of the inflammatory reaction. Therefore, the aim of this study was to examine the effect of Au/TiO_2, Au/ZrO_2 and $Au/Ce/O_2$ on viability, phagocytic capacity and inflammatory profile (TNF-α and IL-1β secretion) of murine macrophages. The most important result of this study is an anti-inflammatory effect of Au/MOx NPs depending on the MOx nature with particle internalization and no alteration of cell viability and phagocytosis. The effect was dependent on the MOx NPs chemical nature (Au/TiO_2> Au/ZrO_2> Au/CeO_2 if we consider the number of cytokines whose concentration was reduced by the NPs), and on the inflammatory mediator considered. The effect of Au/TiO_2 NPs was not related to Au NPs size (at least in the case of Au/TiO_2 NPs in the range of 3-8 nm). To the best of our knowledge, this is the first demonstration of an anti-inflammatory effect of Au/MOx NPs.

INTRODUCTION

Gold (Au) can be deposited as nanoparticles (NPs) smaller than 10 nm in diameter on a variety of metal oxide (MOx) NPs. Au/MOx NPs have attracted much attention due to their high catalytic performance for such as room temperature CO oxidation and selective oxidations in liquid phase[12]. The catalytic activity of Au strongly depends on the kind of support. For example, although TiO_2 is almost inactive for CO oxidation, the deposition of Au NPs onto TiO_2 enables to catalyze CO oxidation at room temperature [34].

These data in the field of heterogeneous catalysis have firmly established that deposition of Au on MOx NPs increases dramatically the intrinsic catalytic activity of these NPs and this could also be the case for the biological activity. For example, Menchon and co-workers [5] reported that Au/CeO_2 exhibits antioxidant activity against reactive oxygen species (ROS) in Hep3B and HeLa cell related lines due to a peroxidase activity. Since the inflammatory reaction is highly dependent on oxidative stress [3], one can hypothesize that, in addition to their antioxidant properties, Au/MOx NPs can have anti-inflammatory effects. Such an effect could have important implications in terms of medical utilization of Au/MOx NPs. However, to the best of our knowledge no data on this effect is available in the current literature.

Therefore, in the present study we examined the effect of Au/MOx on cytotoxic and inflammatory response of macrophages, a key cell type involved in the inflammatory reaction. We used murine macrophages and investigated the roles of the size of Au NPs, the chemical nature of the supporting MOx NPs, and the kinetics of Au/MOx NPs interference with the inflammatory reaction.

RESULTS

No cytotoxic effect of Au/TiO_2 NPs on mouse macrophages

Since physico-chemical properties of Au/TiO_2have already been extensively described [134], we have first compared biological effects of these Au/TiO_2NPs versus TiO_2NPs on mouse peritoneal macrophages. No cytotoxicity was observed by either of MTT (Figure 1a and b) or LDH release assays (Figure 1c and d) for TiO_2 and Au/TiO_2NPs regardless of the concentration (1 to 100 µg.ml^{-1}), the exposure time (24 and 48h) and the size of Au NPs. By contrast, Ag/$TiO_2$and Pt/TiO_2 displayed significant cytotoxic effects in murine RAW 264.7 macrophages at 100 µg.ml^{-1} as compared to TiO_2, whereas Au/TiO_2 and Pd/TiO_2 did not show any cytotoxicity (Figure 2).

$TiO_2$and Au/TiO_2 NPs (50 µg.ml^{-1}, 6h incubation) significantly and similarly increased the phagocytosis of fluorescent beads by peritoneal macrophages, showing an absence of modulation of TiO_2 NPs-induced macrophage activation by AuNPs (Figure 3).

$TiO_2$and Au/TiO_2NP are internalized in mouse peritoneal macrophages

Cellular uptake and intracellular morphology upon 24h exposure to TiO_2 and Au/TiO_2NPs were investigated in ultrathin sections of resin-embedded cells using TEM.

TiO_2NPs and Au/TiO_2NPs (50 $\mu g.ml^{-1}$) were internalized in cells. The prevalent localization of NPs agglomerates was in cell vacuoles (Figure 4 a-c). In accordance with the previous paragraph showing a lack of cytotoxicity, no morphologic sign of cell damage was observed.

No inflammation induced by Au/TiO_2 NPs

Incubation of mouse peritoneal macrophages with TiO_2 NPs (50 $\mu g.ml^{-1}$, 6h), induced a significant increase in the concentration of TNF-α (Figure 5a) and IL-1β (Figure 5b), two main pro-inflammatory cytokines, in cell culture medium. This effect was not observed in the case of Au/TiO_2 NPs without any significant difference between the size of Au NPs (Figure 5).

Au/TiO_2NPsattenuate LPS-induced inflammation

Having demonstrated that Au/TiO_2 NPs did not elicit an inflammatory reaction, we questioned whether Au/TiO_2 NPs could blunt inflammation induced in a model of pathophysiological relevance, such as macrophages exposure to *EscherichiaColi* LPS. Au/TiO_2 having 3 and 8 nm of Au NPs in diameters, abbreviated as Au3/TiO_2 and Au8/TiO_2, respectively, were used. Since no difference of anti-inflammatory effect was observed between Au3/TiO_2 and Au8/TiO_2, we investigated the effects of Au3/TiO_2 NPs (referred to as Au/TiO_2 in the following experiments). Mouse peritoneal macrophages were incubated with culture media 6h (control condition) or LPS 2h, and then the following 4 h with LPS alone or LPS plus TiO_2 or Au/TiO_2. Taking into account the results presented in the previous paragraph, TNF-α and IL-1β cell culture supernatant concentrations were measured as a surrogate of the inflammatory reaction. As expected, incubation of cells with LPS for 2 + 4h induced a significant increase as compared to the control condition ($p<0.05$, Figures 6a and b). Incubation of LPS followed by TiO_2 NPs did not significantly modify the effect of LPS alone. By contrast, this last effect was significantly attenuated by macrophage incubation with Au/TiO_2 NPs ($p<0.05$, Figures 6a and b). These results show that Au/TiO_2 can attenuate LPS induced inflammation, even when cells are incubated with these NPs after incubation with LPS.

Effects of Au/ZrO_2 and Au/CeO_2 NPs on LPS-induced inflammation

After showing the anti-inflammatory effect of Au/TiO_2 NPs, we investigated if this effect was related to the chemical nature of the MOx NPs supports. To answer to this question, we examined the effect of Au NPs deposited on either ZrO_2 or CeO_2 NPs.

No effect was observed with Au/CeO_2 NPs, whereas Au/ZrO_2 NPs attenuated LPS-induced IL-1β production without any effect on TNF-α concentration (Figures 6a and b). Therefore, we can

conclude that Au/MOx NPs possess an anti-inflammatory effect which depends on the nature of the MOx NPs and on the inflammatory mediator examined.

Is the anti-inflammatory effect of Au/MOx NP related to cytokines adsorption on their surface?

We investigated the mechanisms underlining the anti-inflammatory effect of Au/MOx NPs. Since NPs adsorb different proteins on their surfaces [6], we then investigated if the decreased concentration of LPS-induced TNF-α and IL-1β concentration observed with Au/TiO_2 and Au/ZrO_2 (only for IL-1β in this last case) was related to adsorption of these cytokines on these Au/MOx NPs. The results of these experiments showed that incubation of each one of these cytokines with the different Au/MOx NPs examined in this study did not change its respective concentration when compared to the MOx NPs without Au (Figure 7 a and b). This result excludes cytokines adsorption as a mechanism explaining the anti-inflammatory effect of Au/TiO_2 and Au/ZrO_2 NPs.

Is the anti-inflammatory effect of Au/MOx NP related to their antioxidant properties?

We then examined if the anti-inflammatory effect of Au/TiO_2 and Au/ZrO_2 was related to antioxidant properties, as demonstrated in other conditions [78]. To investigate this issue, we measured the effect of Au/MOx NPs on intracellular reactive oxygen species (ROS) concentration. These experiments showed that intracellular ROS production induced by Au/TiO_2 and Au/ZrO_2 NPs was smaller than that of TiO_2 and ZrO_2 respectively, demonstrating an antioxidant effect of these NPs (Table 1), in accordance with their (partial) anti-inflammatory effect. This effect was more important in the case of Au/ZrO_2 compared to Au/TiO_2 (mean reduction of 32% vs 11% compared to ZrO_2 and TiO_2 respectively). This effect could be involved in the anti-inflammatory effect described previously. Interestingly, levels of ROS were lower in cells exposed to CeO_2 as compared to cells exposed to TiO_2 and ZrO_2, in accordance with antioxidant properties of CeO_2 described previously [9].

DISCUSSION

The most important result of this study is an anti-inflammatory effect of Au/MOx NPs depending on the MOx nature with particle internalization and no alteration of cell viability and phagocytosis. Interestingly, the lack of effect Au/TiO_2 on cell viability appears relatively specific for this combination of NPs, since Ag/TiO_2 and Pt/TiO_2 impaired macrophages viability. The effect of Au/TiO_2 NPs was not related to Au NPs size (at least in the case of Au/TiO_2 NPs in the range of 3-8 nm) and was dependent on the MOx NPs chemical nature (Au/TiO_2> Au/ZrO_2> Au/CeO_2 if we consider the number of cytokines whose concentration was reduced by the NPs) and on the inflammatory mediator considered. To the best of our knowledge, this is the first demonstration that Au/MOx present anti-inflammatory properties.

The effect of Au/MOx could be related to anti-inflammatory properties of Au NPs *per se*. Indeed, gold colloids have been thought to cure various diseases for many centuries, and recent studies have demonstrated that this effect is mediated by inhibition of NF-κB activation [10]. Different studies showed a similar effect in the case of Au NPs *in vitro* and *in vivo*, this effect being usually mediated by antioxidant properties [11,12,13,14,15]. However, other studies showed opposite results. For example, Ng and coworkers [16] showed that incubation of human bronchial epithelial cells with 50 $\mu g.ml^{-1}$ of 20 nm Au NPs activated NF-κB in bronchial epithelial cells. Close results were shown in other cell types [17,18]. Therefore, an anti-inflammatory effect of Au NPs *per se* seems not a univocal mechanism explaining the anti-inflammatory effect of Au/MOx NPs. Moreover, attributing our results to the biological activity of Au NPs is questionable since most of the studies showing an effect of Au NPs on inflammation examined concentrations far above the ones to whom cells were exposed in the present study, taking into account that Au NPs represented only 1% of the mass of Au/MOx.

Adsorption of TNF-α and IL-1β on Au/MOx surface could also explain their different anti-inflammatory activity. Indeed, NPs, including Au NPs, can adsorb different molecules on their surface, resulting in their inactivation and reduction in their concentration in the medium [19]. However, this mechanism seems unlikely in the present study since we did not observe any significant difference in TNF-α and IL-1β levels when these cytokines were incubated with TiO_2 or ZrO_2 NPs and their respective Au counterparts.

Finally, the differences in the anti-inflammatory effect of Au/MOx NPs could be related to their different antioxidant properties. However, the anti-inflammatory effect of Au/MOx NPs was not paralleled by the intracellular antioxidant properties since both Au/TiO_2 and Au/ZrO_2 NPs reduced intracellular ROS concentration (with a more important effect of Au/ZrO_2 than Au/TiO_2) whereas only Au/TiO_2 attenuated both TNF-α and IL-1β induction. Moreover, the absence of an anti-inflammatory effect of Au/CeO_2 was paralleled by an absence of an antioxidant effect of this NP as compared to CeO_2 NPs. Interestingly, in concordance with different studies, CeO_2 NPs exerted an antioxidant effect as compared to TiO_2 and ZrO_2 NPs (Table 1), but this effect was not accompanied by an anti-inflammatory effect. Collectively, these data suggest that in contrast with our initial hypothesis, an antioxidant effect does not appear as a mechanism globally explaining the effect of Au/TiO_2 and Au/ZrO_2. Indeed, an antioxidant effect could potentially explain the effect of Au/TiO_2 NPs but not the one of Au/ZrO_2 NPs because these last NPs had showed an antioxidant effect similar to Au/TiO_2but attenuated only IL-1β induction. Consequently, the effect of Au/ZrO_2 appears to depend on pathways inhibiting IL-1β but not TNF-α expression.

Numerous mechanisms control the production and activity of IL-1β, including the processing of the 31-kDa, inactive IL-1β precursor into the bioactive, 17-kDa cytokine *via* intracellular protein complexes termed the inflammasomes [20].The most intensely studied inflammasome is the NLRP3 inflammasome. Various stimuli activate the NLRP3inflammasome: bacterial structures such as muramyl dipeptide or LPS, bacterial RNA, β-glucan, double-stranded RNA, etc. The release of ROS has been repeatedly reported to mediate NLRP3 inflammasome activation by various stimuli, including LPS, but this has been surrounded by controversy [21]. Other proposed mechanisms responsible for NLRP3 inflammasome activation are *i)* translocation to mitochondria [22], *ii)* release of mitochondrial DNA or cardiolipin [23], *iii)* release of lysosomal cathepsins into the cytoplasm [24], or iv) calcium-dependent phospholipase 2 activation [20]. Interference with one or several mechanisms could explain attenuation of LPS-induced IL-1β expression by Au/ZrO_2 NPs. However, investigating these possibilities needs further studies.

This study presents 2 main limitations. First, we only measured 2 cytokines as a surrogate of inflammatory markers. Even if these cytokines are broadly representative of the inflammatory reaction and are one of the very early ones in the inflammatory cascade, and we investigate primary murine macrophages (a key cell involved in inflammation), a wider analysis of mediators of this reaction is necessary to validate the present results. Second, we investigated only 3 MOx NPs supports. Although we choose supports widely characterized in terms of catalytic properties when combined with Au NPs, investigating a broader panel of MOx could allow a better characterizing the anti-inflammatory properties of Au/MOx NPs. It has to be noted, however, that we compared cytotoxicity of Au/TiO_2 with other metallic NPs deposited on TiO_2 (Ag, Pt and Pd) and we showed that only Au/TiO_2 and Pd/TiO_2 did not impaired cell viability at the concentrations examined, providing an additional argument for the beneficial effects of Au/TiO_2 NPs.

In conclusion, this study showed that Au/MOx possess anti-inflammatory properties in macrophages. This effect could have potential applications in the clinical setting since it does not interfere with physiological parameters of these cells such as viability and phagocytosis.

METHODS

Nanoparticles preparation

Au NPs with two different mean diameters (3 and 8 nm) supported on pristine TiO_2 NPs (Nippon Aerosil Co., Ltd., AEROXIDE P25) were prepared, termed $Au3/TiO_2$ and $Au8/TiO_2$, respectively. $Au3/TiO_2$ were prepared by deposition-precipitation[3] followed by calcination at 300 °C for 4h. $Au8/TiO_2$ was prepared by solid grinding with dimethyl Au (III) acetylacetonate and by calcination at 300 °C[25]. Au/ZrO_2 and Au/CeO_2 were purchased from Haruta Gold Inc©. The primary particle sizes of

Au3/TiO_2, Au/ZrO_2, and Au/CeO_2were 26 nm, 11 nm, and 7.3 nm respectively, estimated from their specific surface areas of the MOx NPs. The secondary particle sizes of Au3/TiO_2, Au/ZrO_2, and Au/CeO_2 were 5.5 µm, 0.9 µm, and 3.6 µm respectively, determined by dynamic light scattering method. Using atomic absorption spectroscopy, the actual Au loadings for Au3/TiO_2, Au8/TiO_2, Au/ZrO_2, and Au/CeO_2 were 0.96, 1.18, 0.97, and 0.96 wt%, respectively. The mean diameters of Au NPs were estimated by high-angle annular dark-field scanning transmission electron microscopy (HAADF-STEM) to be 3.3±1.4 nm for Au3/TiO_2, 7.8±2.7 nm for Au8/TiO_2, and 3.3±1.8 nm for Au/ZrO_2. In the case of Au/CeO_2, it was difficult to observe Au NPs because Au was mostly deposited as single atoms and the atomic number of Ce is close to that of Au.

Metal NPs other than Au, namely Ag, Pt, Pd, supported on TiO_2 (loading: 1wt%) were prepared by impregnation. TiO_2 was suspended in aqueous $AgNO_3$, $H_2PtCl_6{\cdot}6H_2O$, or $PdCl_2$, followed by evaporation to dryness at 70 °C. The remaining paste was reduced in 10% H_2 in N_2at 300 °C for 4h.

Cells isolation and incubation with nanoparticles

Peritoneal macrophages and macrophages from the RAW 264.7 cell line were used in the different experiments.

Peritoneal macrophages.C57BL/6 mice were injected intraperitoneally with 1 ml of 3% Brewer thioglycollate (Sigma-Aldrich, B2551). After 96 h, peritoneal cells were harvested by lavage with 0.67% phosphate buffered saline (PBS). After a soft centrifugation, cells were maintained in Dulbecco's modified Eagle medium (DMEM) 4,5 $g.L^{-1}$ glucose supplemented with 10 % fetal calf serum (FCS)and 1 % penicillin and 1% streptomycin. Then mice peritoneal macrophagic cells were exposed for 6–48 h to 1–100 µg/mL particles of Au/TiO_2, Au/ZrO_2, Au/CeO_2, and MOx alone.

RAW 264.7 macrophages. The RAW 264.7 cells were cultured using a medium having the same composition as above and were exposed for 24 h to 1–100 µg/ml nanoparticles of Au/TiO_2, Ag/TiO_2, Pt/TiO_2, Pd/TiO_2 and TiO_2.

Cellular viability

The viability of cells was measured by 3-[4,5-dimethylthiazol-2-yl]-2,5 diphenyl tetrazolium bromide (MTT) assay, 2-(4-iodophenyl)-3-(4-nitrophenyl)-5-(2,4-disulfophenyl)-2H-tetrazolium, monosodium salt (WST-1) assay, and the quantification of the release of lactate dehydrogenase (LDH).

Phagocytosis assay

RAW 264.7 cells (ATCC) were exposed to 50 $\mu g.mL^{-1}$ CNT for 6 h, together with Latex beads-rabbit IgG-FITC complex, as per the manufacturer's instructions (Phagocytosis assay Kit; Cayman Chemical, 500,290). Fluorescence was measured at λexc = 485 nm, and λemi = 535 nm [26].

Transmission electron microscopy (TEM)

Macrophages submitted to different exposure were fixed overnight at 4 °C using TEM-grade fixative solution of 2% formaldehyde and 2.5% glutaraldehyde in 0.1 M sodium cacodylate buffer, pH 7.4. The samples were washed and stored in 0.1 M sodium cacodylate buffer and kept at 4 °C until processing. Sample embedding was performed in epoxy resin according a standard protocol.

Inflammatory responses

Inflammatory response was evaluated by the quantification of cytokines such as tumor necrosis factor (TNF)-α and interleukin (IL)-1β in cell supernatant, measured by enzyme-linked immunosorbent assay (ELISA).

Measurement of oxidative stress by DCFH-DA assay

Endogenous ROS were quantified by oxidation of 2',7'-dichlorofluorescin diacetate (DCFH-DA) into 2',7'-dichlorofluorescin (Sigma, Saint Quentin Fallavier, France). Briefly, cells were cultivated in six-well culture plates and treated with 50µg.ml^{-1} NPs. Cells were also treated with 250 µM H_2O_2 as a positive control (data not shown). Cells were incubated with 20 µM DCFH-DA for 30 min at 37 °C and fluorescence recorded for 90 min. Results were expressed as the mean ratio of fluorescence recorded every 15 min during the 90 min period.

Measurement of TNF-α and IL-1β adsorption to NPs

Adsorption of TNF-α and IL-1β adsorption to NPs was performed by ELISA as described previously described [27].

Statistical Analysis

JASP software (version 0.11.1, https://jasp-stats.org/) was used to analyze quantitative data. Non-parametric ANOVA was used to compare multiple groups. Paired comparisons with Mann-Whitney test were performed if the differences using ANOVA were statistically significantly different. Data were presented as mean values ± standard error of the mean (SEM), and results were considered statistically significant if $p< 0.05$.

Study approval for animal experiments

The Institutional Animal Care and Use Committee approved experimental procedures on mice (Autorisation De Projet Utilisant Des Animaux A Des Fins Scientifiques APAFIS authorization #14914-2018042515599016). All experiments were carried out in accordance with relevant guidelines and regulations. The study was carried out in compliance with the ARRIVE guidelines.

DATA AVAILABILITY

The datasets used and/or analyzed during the current study are available from the corresponding author on reasonable request.

REFERENCES

1 Haruta, M. When gold is not noble: catalysis by nanoparticles. *Chem Rec***3**, 75-87, doi:10.1002/tcr.10053 (2003).

2 Taketoshi, A. & Haruta, M. Size- and Structure-specificity in Catalysis by Gold Clusters. *Chem Lett***43**, 380-387, doi:10.1246/cl.131232 (2014).

3 Haruta, M. *et al.* Low-Temperature Oxidation of Co over Gold Supported on Tio2, Alpha-Fe2o3, and Co3o4. *J Catal***144**, 175-192, doi:DOI 10.1006/jcat.1993.1322 (1993).

4 Ishida, T., Murayama, T., Taketoshi, A. & Haruta, M. Importance of Size and Contact Structure of Gold Nanoparticles for the Genesis of Unique Catalytic Processes. *Chem Rev***120**, 464-525, doi:10.1021/acs.chemrev.9b00551 (2020).

5 Menchon, C. *et al.*Gold nanoparticles supported on nanoparticulate ceria as a powerful agent against intracellular oxidative stress. *Small***8**, 1895-1903, doi:10.1002/smll.201102255 (2012).

6 Lundqvist, M. *et al.* Nanoparticle size and surface properties determine the protein corona with possible implications for biological impacts. *Proc Natl Acad Sci U S A***105**, 14265-14270, doi:0805135105 10.1073/pnas.0805135105 (2008).

7 Lucchetti, B. F. C. *et al.* Metabolic syndrome agravates cardiovascular, oxidative and inflammatory dysfunction during the acute phase of Trypanosoma cruzi infection in mice. *Sci Rep***9**, 18885, doi:10.1038/s41598-019-55363-9 (2019).

8 Scalavino, V. *et al.* miR-369-3p modulates inducible nitric oxide synthase and is involved in regulation of chronic inflammatory response. *Sci Rep***10**, 15942, doi:10.1038/s41598-020-72991-8 (2020).

9 Pezzini, I. *et al.* Cerium oxide nanoparticles: the regenerative redox machine in bioenergetic imbalance. *Nanomedicine (Lond)***12**, 403-416, doi:10.2217/nnm-2016-0342 (2017).

10 Narayanan, K. B. & Park, H. H. Pleiotropic functions of antioxidant nanoparticles for longevity and medicine. *Adv Colloid Interface Sci***201-202**, 30-42, doi:10.1016/j.cis.2013.10.008 (2013).

11 Zhu, S. *et al.*Orally administered gold nanoparticles protect against colitis by attenuating Toll-like receptor 4- and reactive oxygen/nitrogen species-mediated inflammatory responses but could induce gut dysbiosis in mice. *J Nanobiotechnology***16**, 86, doi:10.1186/s12951-018-0415-5 (2018).

12 Lai, T. H., Shieh, J. M., Tsou, C. J. & Wu, W. B. Gold nanoparticles induce heme oxygenase-1 expression through Nrf2 activation and Bach1 export in human vascular endothelial cells. *Int J Nanomedicine***10**, 5925-5939, doi:10.2147/IJN.S88514 (2015).

13 Pereira, D. V. *et al.* Effects of gold nanoparticles on endotoxin-induced uveitis in rats. *Invest Ophthalmol Vis Sci***53**, 8036-8041, doi:10.1167/iovs.12-10743 (2012).

14 Haupenthal, D. *et al.*Effects of chronic treatment with gold nanoparticles on inflammatory responses and oxidative stress in Mdx mice. *J Drug Target*, 1-9, doi:10.1080/1061186X.2019.1613408 (2019).

15 Taratummarat, S. *et al.* Gold nanoparticles attenuates bacterial sepsis in cecal ligation and puncture mouse model through the induction of M2 macrophage polarization. *BMC Microbiol***18**, 85, doi:10.1186/s12866-018-1227-3 (2018).

16 Ng, C. T. *et al.* Gold nanoparticles induce serum amyloid A 1-Toll-like receptor 2 mediated NF-kB signaling in lung cells in vitro. *Chem Biol Interact***289**, 81-89, doi:10.1016/j.cbi.2018.04.022 (2018).

17 Khan, H. A., Abdelhalim, M. A., Alhomida, A. S. & Al Ayed, M. S. Transient increase in IL-1beta, IL-6 and TNF-alpha gene expression in rat liver exposed to gold nanoparticles. *Genet Mol Res***12**, 5851-5857, doi:10.4238/2013.November.22.12 (2013).

18 Li, Y. *et al.* Bacterial endotoxin (lipopolysaccharide) binds to the surface of gold nanoparticles, interferes with biocorona formation and induces human monocyte

inflammatory activation. *Nanotoxicology***11**, 1157-1175, doi:10.1080/17435390.2017.1401142 (2017).

19 Mukherjee, P. *et al.* Antiangiogenic properties of gold nanoparticles. *Clin Cancer Res***11**, 3530-3534, doi:10.1158/1078-0432.CCR-04-2482 (2005).

20 Lamkanfi, M. & Dixit, V. M. Mechanisms and functions of inflammasomes. *Cell***157**, 1013-1022, doi:10.1016/j.cell.2014.04.007 (2014).

21 Netea, M. G., van de Veerdonk, F. L., van der Meer, J. W., Dinarello, C. A. & Joosten, L. A. Inflammasome-independent regulation of IL-1-family cytokines. *Annu Rev Immunol***33**, 49-77, doi:10.1146/annurev-immunol-032414-112306 (2015).

22 Subramanian, N., Natarajan, K., Clatworthy, M. R., Wang, Z. & Germain, R. N. The adaptor MAVS promotes NLRP3 mitochondrial localization and inflammasome activation. *Cell***153**, 348-361, doi:10.1016/j.cell.2013.02.054 (2013).

23 Nakahira, K. *et al.* Autophagy proteins regulate innate immune responses by inhibiting the release of mitochondrial DNA mediated by the NALP3 inflammasome. *Nat Immunol***12**, 222-230, doi:10.1038/ni.1980 (2011).

24 Duewell, P. *et al.* NLRP3 inflammasomes are required for atherogenesis and activated by cholesterol crystals. *Nature***464**, 1357-1361, doi:10.1038/nature08938 (2010).

25 Ishida, T. *et al.* Influence of the Support and the Size of Gold Clusters on Catalytic Activity for Glucose Oxidation. *Angew Chem Int Edit***47**, 9265-9268, doi:10.1002/anie.200802845 (2008).

26 Cohignac, V. *et al.* Carbon nanotubes, but not spherical nanoparticles, block autophagy by a shape-related targeting of lysosomes in murine macrophages. *Autophagy***14**, 1323-1334, doi:10.1080/15548627.2018.1474993 (2018).

27 Bussy, C. *et al.* Critical role of surface chemical modifications induced by length shortening on multi-walled carbon nanotubes-induced toxicity. *Part Fibre Toxicol***9**, 46, doi:10.1186/1743-8977-9-46 (2012).

ACKNOWLEDGMENTS

AUTHORS CONTRIBUTION

TF prepared and analyzed NPs, performed chemical experiments and critically reviewed the manuscript. TF, MZ and DE performed biological experiments. TM, MH, and SL critically reviewed the manuscript and worked on its final elaboration. TI contributed to the design of the study, critically reviewed the manuscript and worked on its final elaboration. JB designed the study and wrote the first and final drafts of the manuscript.

All authors approved the final version of the manuscript.

COMPETING INTERESTS

The authors declare no competing interests.

Figure Legends

Figure 1. Cytotoxicity of Au nanoparticles (NPs) with two different diameters (3 and 8 nm respectively) supported on pristine TiO_2 ($Au3/TiO_2$ and $Au8/TiO_2$ respectively) and TiO_2 NPs alone on mouse peritoneal macrophages. Cell viability was measured using the MTT assay (panels a and b) and LDH relargage (panels c and d) after 24 and 48h incubation (panels a and c and b and d respectively). Data are expressed as percentage of control condition (without NPs, 100% is the reference value) and are represented as mean ± SEM of 6 independent experiments. Positive controls are doxorubicine (DOXO, 1, 5 and 10 $\mu g.ml^{-1}$) and TritonX-100 (10 vol. %). * significantly different from control ($p < 0.05$).

Figure 2. Cytotoxicity of Au, Ag, Pt, Pd NPs supported on pristine TiO_2 NPs and pristine TiO_2 NPs alone on murine RAW 264.7 macrophages. Cell viability was measured using the WST-1 assay after 24 h incubation. Data are expressed as percentage of control condition (without NPs, 100% is the reference value) and are represented as mean ± SEM of 6 independent experiments. Positive control is cisplatin (1, 5 and 10 $\mu g.ml^{-1}$). * significantly different from control ($p < 0.05$), $^{\#}$ significantly different from control ($p < 0.01$)

Figure 3. Effect of $Au3/TiO_2$, $Au8/TiO_2$ and TiO_2NPs (50 $\mu g.ml^{-1}$, 6h incubation) on phagocytosis of fluorescent beads by mouse peritoneal macrophages. Data are expressed as arbitrary units (AU) of fluorescence intensity and are represented as mean ± SEM of 6 independent experiments. * significantly different from control ($p < 0.05$).

Figure 4. Transmission electron microscopy views of mouse peritoneal macrophages incubated 24h with 50 $\mu g.ml^{-1}$ of $Au3/TiO_2$, $Au8/TiO_2$ and TiO_2 NPs.

The scale bar in images in column a is 2 microns, and in columns b and c is 0.2 microns. As observed in the images, the prevalent localization of NPs agglomerates was in cell vacuoles. No morphologic sign of cell damage was observed.

Figure 5. Effect of $Au3/TiO_2$, $Au8/TiO_2$ and TiO_2NPs (50 $\mu g.ml^{-1}$, 6h incubation) on TNF-α and IL-1β secretion by mouse peritoneal macrophages (panels a and b respectively). Data are expressed as picograms/ml in cell culture medium and are represented as mean ± SEM of 6 independent experiments. $^{\#}$ significantly different from control ($p < 0.01$)

Figure 6. Effect of Au deposited on different metal oxide NPs on LPS induced TNF-$\alpha$and IL-1β secretion by mouse peritoneal macrophages (Panels a and b respectively). Cells were incubated with culture media 6h (control condition, C) or LPS 2h, and then the following 4 h with LPS alone or LPS plus the different NPs (50 $\mu g.ml^{-1}$). * significantly different from C ($p<0.05$), ** significantly different from LPS 2h – TiO_2 4h ($p< 0.05$), $^{\&}$ significantly different from LPS 2h – ZrO_2 4h($p < 0.05$)

Figure 7. TNF-α and IL-1β adsorption on Au deposited on different metal oxide NPs. NPs (50 $\mu g.ml^{-1}$) were incubated during 6h with TNF-α (150 $pg.ml^{-1}$) and IL-1β (100 $pg.ml^{-1}$) in culture media, then the cytokines were quantified in the media after centrifugation.

Table 1

Nanoparticle	Mean values ± SEM	Statistical significance
Au/TiO_2	12068 ± 499	*
TiO_2	13547 ± 340	
Au/ZrO_2	9170 ± 109	**
ZrO_2	13538 ± 129	
Au/CeO_2	12743 ± 340	
CeO_2	12583 ± 255	#

Reactive oxygen species (ROS) production in RAW 264.7 cells after expositions to different NPs (n=7). The final concentration of NPs was 50 $\mu g.ml^{-1}$. Amounts of ROS production were evaluated by the CM_2-DCFDA. * $p<0.05$ vs TiO_2, ** $p<0.01$ vs ZrO_2, # $p<0.05$ vs TiO_2 and ZrO_2.

Figures

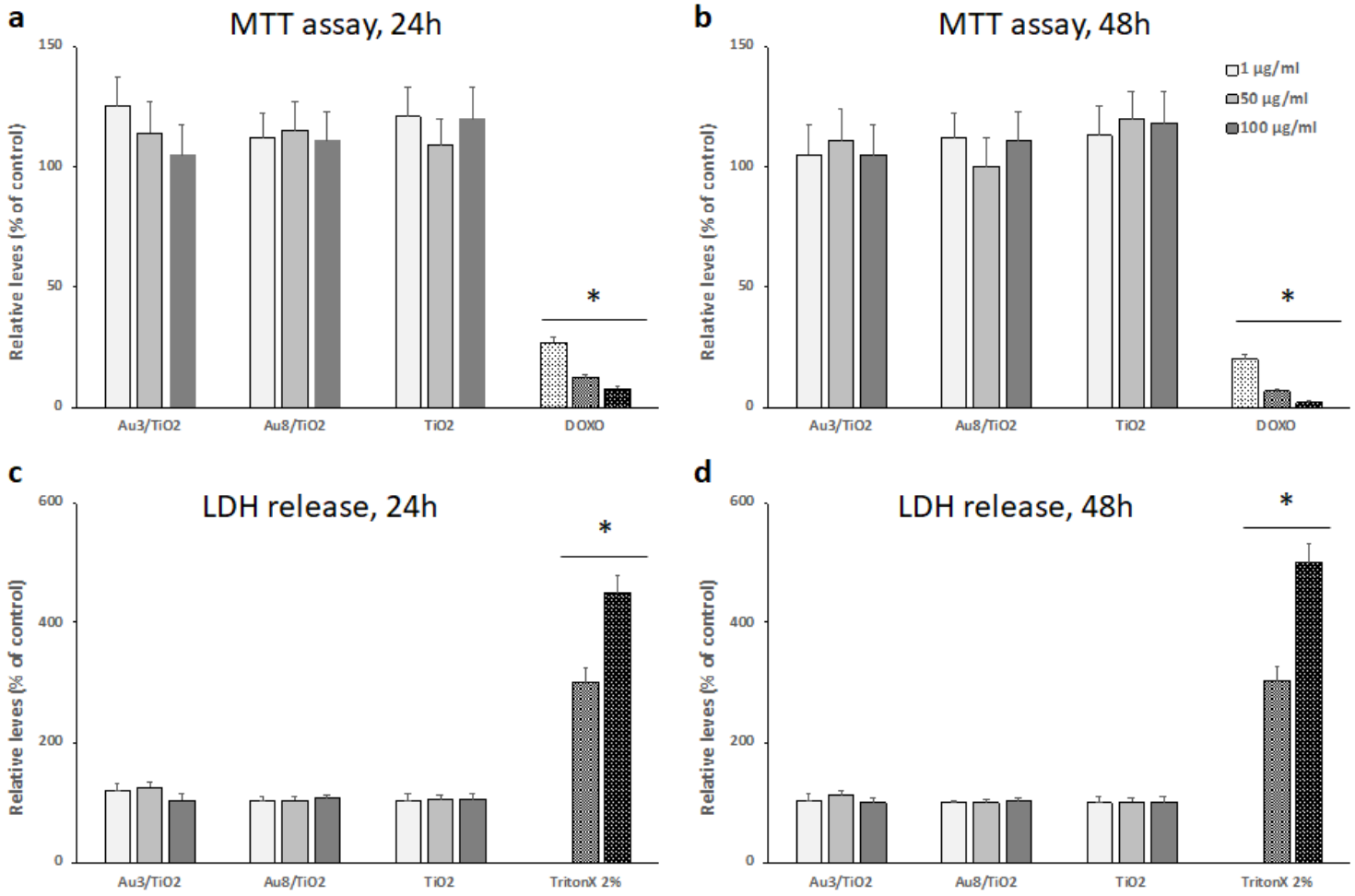

Figure 1

Cytotoxicity of Au nanoparticles (NPs) with two different diameters (3 and 8 nm respectively) supported on pristine TiO2 (Au3/TiO2 and Au8/TiO2 respectively) and TiO2 NPs alone on mouse peritoneal macrophages. Cell viability was measured using the MTT assay (panels a and b) and LDH relargage (panels c and d) after 24 and 48h incubation (panels a and c and b and d respectively). Data are expressed as percentage of control condition (without NPs, 100% is the reference value) and are represented as mean ± SEM of 6 independent experiments. Positive controls are doxorubicine (DOXO, 1, 5 and 10 µg.ml-1) and TritonX-100 (10 vol. %). * significantly different from control ($p < 0.05$).

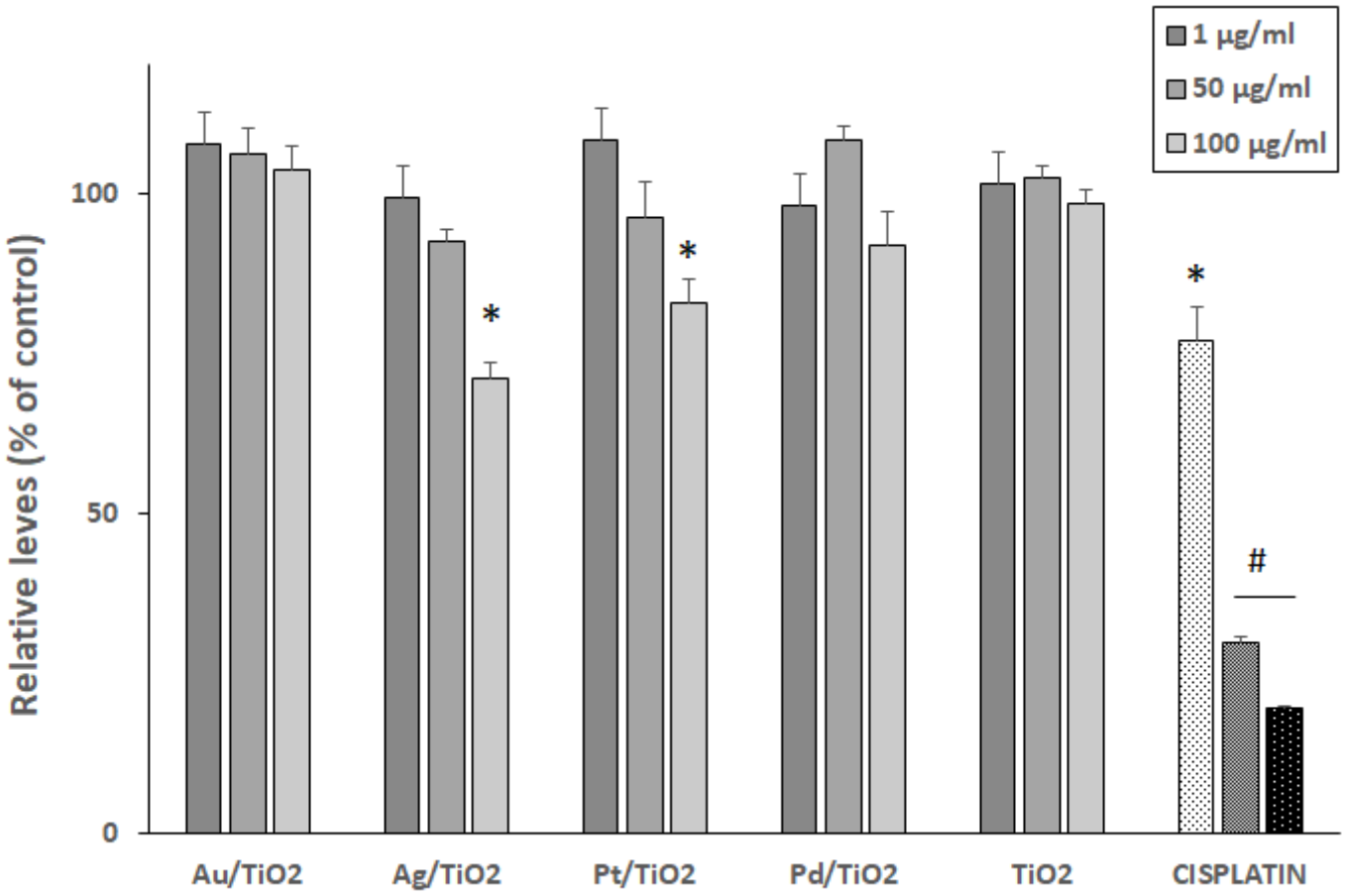

Figure 2

Cytotoxicity of Au, Ag, Pt, Pd NPs supported on pristine TiO2 NPs and pristine TiO2 NPs alone on murine RAW 264.7 macrophages. Cell viability was measured using the WST-1 assay after 24 h incubation. Data are expressed as percentage of control condition (without NPs, 100% is the reference value) and are represented as mean ± SEM of 6 independent experiments. Positive control is cisplatin (1, 5 and 10 µg.ml-1). * significantly different from control ($p < 0.05$), # significantly different from control ($p < 0.01$)

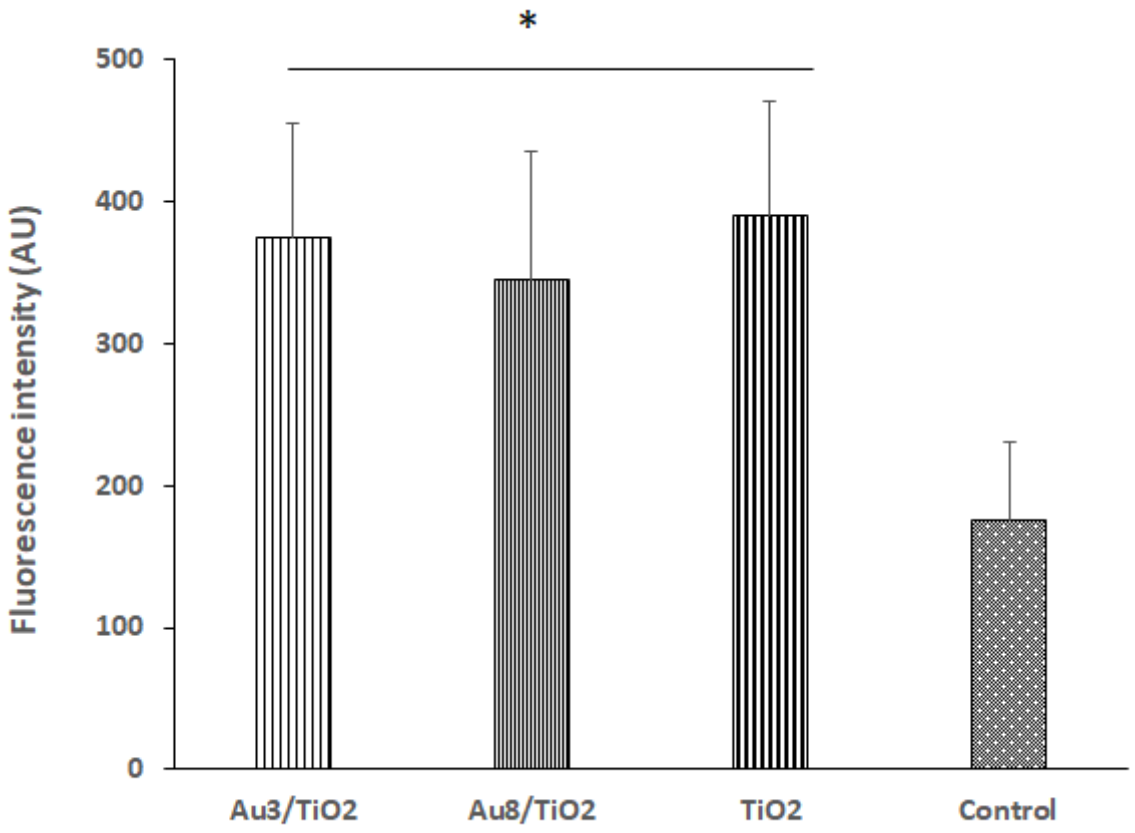

Figure 3

Effect of Au3/TiO2, Au8/TiO2 and TiO2NPs (50 µg.ml-1, 6h incubation) on phagocytosis of fluorescent beads by mouse peritoneal macrophages. Data are expressed as arbitrary units (AU) of fluorescence intensity and are represented as mean ± SEM of 6 independent experiments. * significantly different from control ($p < 0.05$).

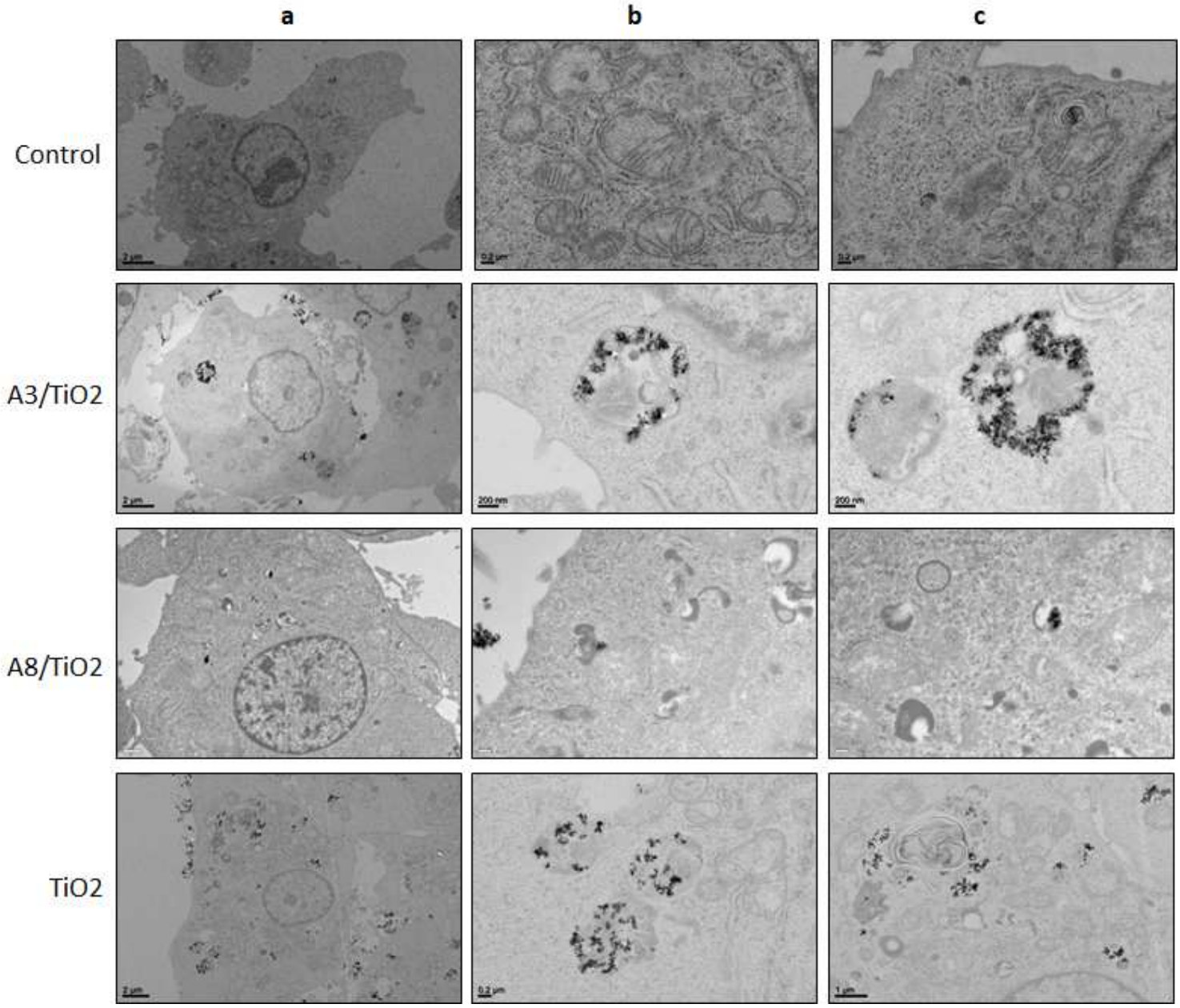

Figure 4

Transmission electron microscopy views of mouse peritoneal macrophages incubated 24h with 50 µg.ml-1 of Au3/TiO2, Au8/TiO2 and TiO2 NPs. The scale bar in images in column a is 2 microns, and in columns b and c is 0.2 microns. As observed in the images, the prevalent localization of NPs agglomerates was in cell vacuoles. No morphologic sign of cell damage was observed.

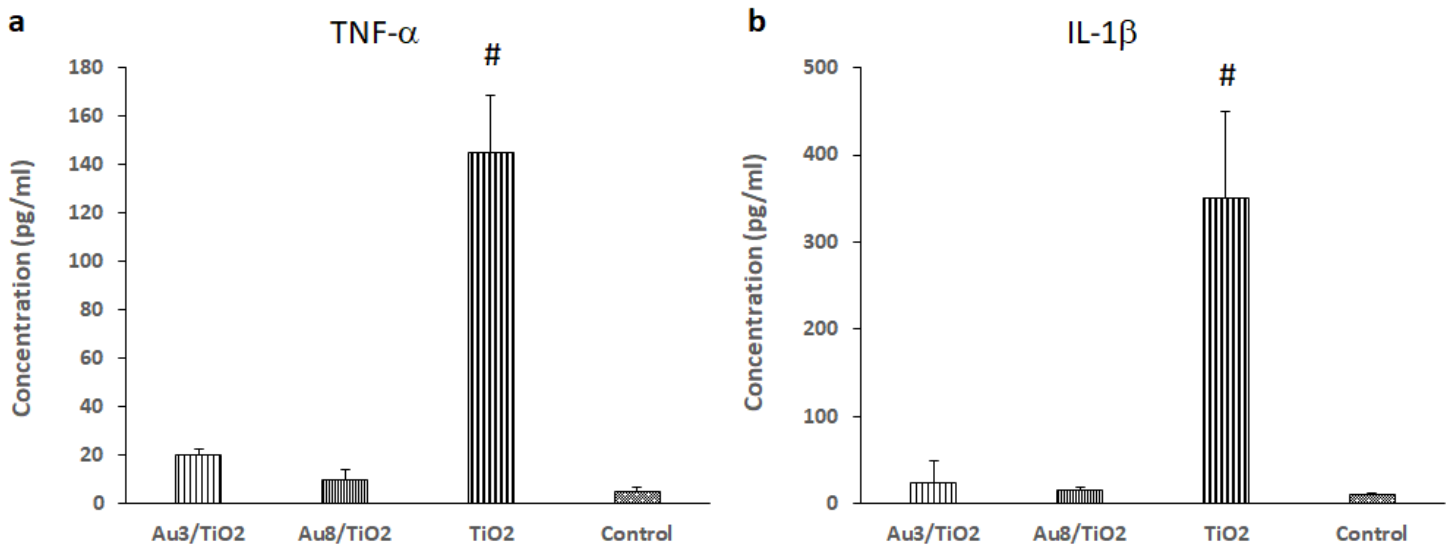

Figure 5

Effect of Au3/TiO2, Au8/TiO2 and TiO2NPs (50 µg.ml-1, 6h incubation) on TNF-α and IL-1β secretion by mouse peritoneal macrophages (panels a and b respectively). Data are expressed as picograms/ml in cell culture medium and are represented as mean ± SEM of 6 independent experiments. # significantly different from control ($p < 0.01$)

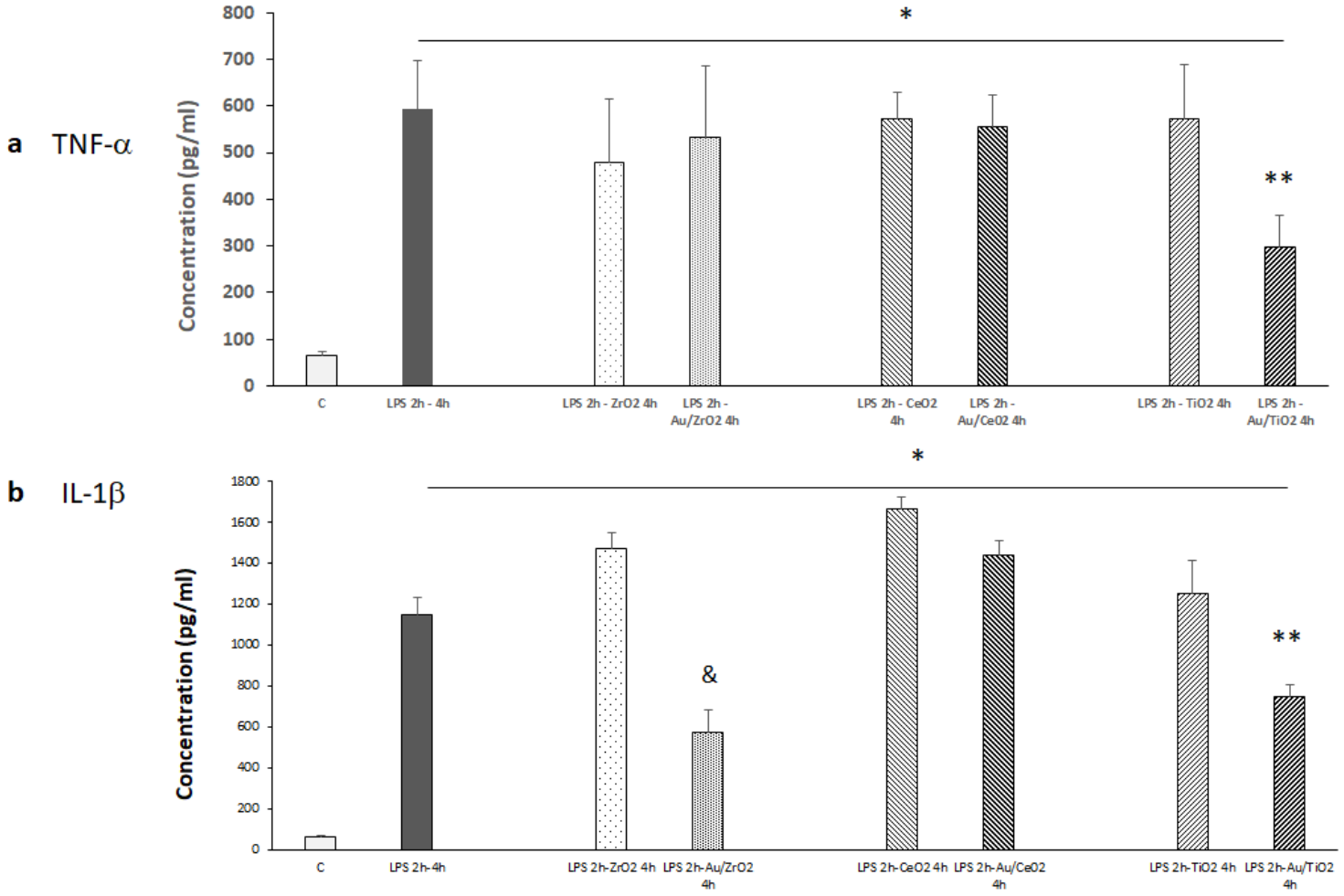

Figure 6

Effect of Au deposited on different metal oxide NPs on LPS induced TNF-α and IL-1β secretion by mouse peritoneal macrophages (Panels a and b respectively). Cells were incubated with culture media 6h (control condition, C) or LPS 2h, and then the following 4 h with LPS alone or LPS plus the different NPs (50 µg.ml-1). * significantly different from C ($p<0.05$), ** significantly different from LPS 2h – TiO2 4h ($p< 0.05$), & significantly different from LPS 2h – ZrO2 4h($p < 0.05$)

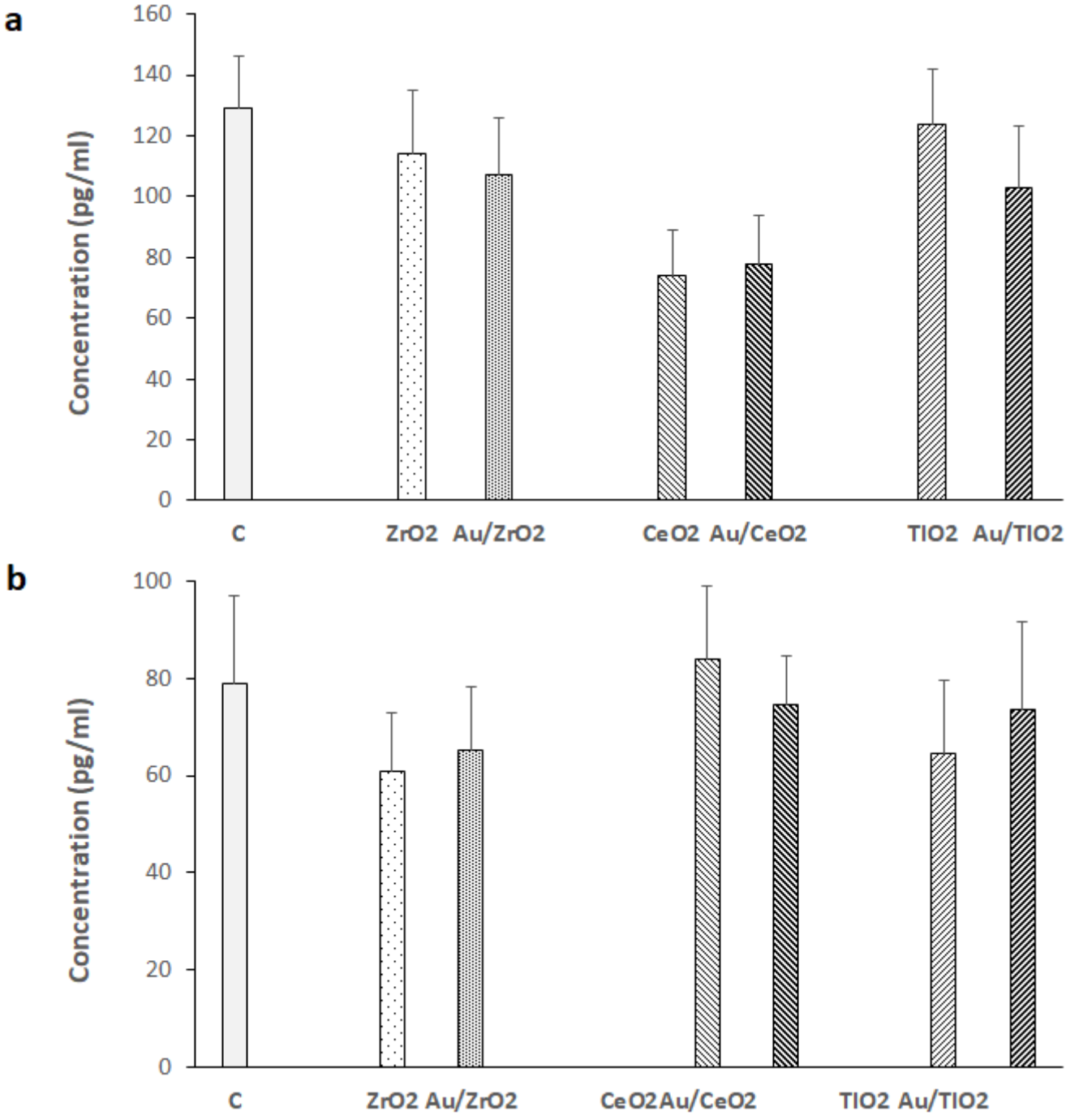

Figure 7

TNF-α and IL-1β adsorption on Au deposited on different metal oxide NPs. NPs (50 µg.ml-1) were incubated during 6h with TNF-α (150 pg.ml-1) and IL-1β (100 pg.ml-1) in culture media, then the cytokines were quantified in the media after centrifugation.